

 <p>ISSN NO. 2320-5407</p>	<p>Journal Homepage: - <a href="http://www.journalijar.com">www.journalijar.com</a></p> <h2>INTERNATIONAL JOURNAL OF ADVANCED RESEARCH (IJAR)</h2> <p>Article DOI: 10.21474/IJAR01/12209 DOI URL: <a href="http://dx.doi.org/10.21474/IJAR01/12209">http://dx.doi.org/10.21474/IJAR01/12209</a></p>	 <p>INTERNATIONAL JOURNAL OF ADVANCED RESEARCH (IJAR) ISSN 2320-5407 Journal Homepage: <a href="http://www.journalijar.com">http://www.journalijar.com</a> Journal DOI: 10.21474/IJAR01</p>
---	---	--

### RESEARCH ARTICLE

## SYNTHESIS, CHARACTERIZATION AND PHOTOLUMINESCENCE PROPERTIES OF EU<sup>3+</sup> DOPED CALCIUM SILICATE PHOSPHOR BY CONVENTIONAL SOLID STATE REACTION METHOD

Ch. Atchyutha Rao<sup>1</sup> and K.V.R. Murthy<sup>2</sup>

1. Department of Physics, Bapatla College of Arts and Sciences, Bapatla - 522101, A.P, India.
2. Display Materials Laboratory, Applied Physics Department, Faculty of Technology and Engineering, M. S. University of Baroda, Vadodara-390001, India.

#### Manuscript Info

##### Manuscript History

Received: 20 October 2020

Final Accepted: 24 November 2020

Published: December 2020

##### Key words:-

Calcium Silicate phosphor, Rare earth ion, Conventional Solid state reaction method

#### Abstract

Calcium Silicate phosphor acquires a higher luminous efficiency when it is doped with rare earth activated ions. Silicate phosphors are used for a fluorescent, a cathode-ray tube, a luminous body, a vacuum ultraviolet excitation light emitting element etc. The silicates of calcium are known for their thermal stability, high temperature strength, low thermal expansion, cheap residence and chemical inertness. The present paper reports on the synthesis, characterization and photoluminescence properties of Eu<sup>3+</sup> doped calcium silicate phosphor prepared by conventional solid state reaction method heating at 1200<sup>o</sup>C for 3 hrs. The received cakes are grounded for 30 minutes each. The phosphors are prepared and the received powder is subjected to PL, XRD, SEM, EDAX and CIE analysis. The following section discusses and the experimental results are mentioned in these phosphors. The present Phosphor can act as a host for red light emission in many display devices and technological applications.

Copy Right, IJAR, 2020,. All rights reserved.

#### Introduction:-

Recently, rare earth incorporated silicate lattice based phosphors have attracted significant interest on the basis of their stable crystal structure, excellent physical and chemical stability, water resistant property, low cost and potential to yield better luminescence. Rare earths are the most common activator ions used for doping in the phosphor materials due to their 4f→4f and 5d→4f transitions. Specially, Eu<sup>3+</sup> ions has been used as an effective activator as it emits an intense red color in 610-625nm region and shows characteristic emission lines due to <sup>5</sup>D<sub>0</sub>→<sup>7</sup>F<sub>J</sub> (J = 0-4) transitions [1-10]. In addition to the common properties of rare earth elements, Europium, a special element in the lanthanides, displays the property of valence fluctuation – with divalent or trivalent valence state. Europium also exhibits different luminescence characteristics due to different valences. The emission spectrum of Eu<sup>3+</sup> ions (electronic configuration <sup>4</sup>f<sub>6</sub>) shows emission lines extending from visible region to the near infrared. Eu<sup>3+</sup> doped phosphors have been developed as a new generation of red emitting materials because of their wide applicability in light emitting diodes, fluorescent tubes, flat panel display, mercury free lamps, color television displays and other electronic devices. Silicates of Mg, Ca, Sr and Ba are the brilliant luminescent host as they possess some remarkable characteristics such as high temperature strength, low thermal expansion, conductivity and suitable lattice sites for incorporation of rare earth and transition metal ions [11-14]. Eu<sup>3+</sup> ions are extensively used in electroluminescence panels (EL), plasma display panels (PDP), higher efficiency fluorescent lamps etc since they are important emitters in the red region of the visible spectrum. The current phosphor research is focused on the

**Corresponding Author:- Ch. Atchyutha Rao**

Address:- Department of Physics, Bapatla College of Arts and Sciences, Bapatla - 522101, A.P, India.

development of novel and efficient light emitting materials having high luminescence efficiency and good thermal as well as chemical stability. The selection of trivalent europium doped Calcium silicate phosphor host is important from practical point of view also because  $\text{Eu}^{3+}$  easily substitute  $\text{Y}^{3+}$  ion from the host lattice and thus improves the luminescence property and stability of materials. Energy transfer occurs from sensitizer to the activator ion in tricolor phosphor systems [15, 16]. Solid state reaction method was used to explore these light emitting materials which require high temperature. Red color is essential for generating high coloration index and low correlated color temperature important for the lighting applications.

### Experimental:

#### Material preparation:

The  $\text{Ca}_2\text{Si}_3\text{O}_8:\text{Eu}^{3+}$  phosphor was prepared by the high temperature conventional Solid state reaction method. The raw materials are calcium carbonate [ $\text{CaCO}_3$  (assay-99.90%)], Silicon di-oxide [ $\text{SiO}_2$  (assay-99.99%)] and Europium oxide [ $\text{Eu}_2\text{O}_3$  (assay-99.99%)] Sigma-Aldrich Chemie, Inc, Germany, all of analytical grade (A.R.), were weighed according to the compositions in the following reaction  $2\text{CaCO}_3 + 3\text{SiO}_2 \longrightarrow \text{Ca}_2\text{Si}_3\text{O}_8 + 2\text{CO}_2\uparrow$ . Initially, the raw materials were weighed according to the nominal compositions of  $\text{Ca}_2\text{Si}_3\text{O}_8:\text{Eu}^{3+}$  phosphor. Then the powders were mixed and milled thoroughly for 3 hrs using mortar and pestle. The grinded sample was placed in an alumina crucible and subsequently fired at  $1200^\circ\text{C}$  for 3 hrs in air. At last the nominal compounds were obtained after the cooling down of programmable muffle furnace with a heating/cooling rate of  $5^\circ\text{C}/\text{min}$ . Finally the samples were allowed to cool down to room temperature for about 20hrs. All the samples were again ground into fine powder about an hour.

#### Characterization Techniques:

The phase structure, crystallite size, particle size, surface morphology, elemental analysis, different stretching mode was analyzed by X-ray diffractometer (XRD), Field emission scanning electron microscopy (FESEM) and Energy-dispersive X-ray spectroscopy (EDS, EDX, EDXS, or XEDS), sometimes called energy dispersive X-ray analysis (EDXA) or energy dispersive X-ray microanalysis (EDXMA), is an analytical technique used for the elemental analysis or chemical characterization of samples respectively.

The structural studies were carried out by X-ray diffraction technique in reflection mode with filtered Cu K $\alpha$  radiation ( $\lambda = 1.54051 \text{ \AA}$ ) with Rigaku, D Max III VC, Japan. Raman spectra were recorded on Reni show In via Raman microscope. PL measurements of the emission and the excitation spectra of the synthesized powders were characterized with a spectrofluorophotometer (Shimadzu RF 5301 PC) with xenon lamp as excitation source [17, 18]. All the spectra were recorded at room temperature. Emission and excitation spectra were recorded using a spectral slit width of 1.5nm. The morphologies (SEM) of the phosphor powders were obtained by using the Nova NanoSEM450. The Commission International de l'Eclairage (CIE-1931 Colour Chart) co-ordinates were calculated by the spectrophotometric method using the spectral energy distribution. The chromatic coordinates (x, y) of prepared materials were calculated with colour calculator version 2, software from Radiant Imaging.

### Results and Discussions:-

#### XRD Analysis:

In order to determine the phase structure, powder XRD analysis has been carried out. The typical XRD patterns of  $\text{Ca}_2\text{Si}_3\text{O}_8:\text{Eu}^{3+}$  (0.5mol %) phosphor with the standard XRD pattern is shown in Figure.1. From the XRD patterns it looks phosphors may not be in single phase since the sintering temperature need for silicate phosphors is  $1300^\circ\text{C}$  because the lack of the experimental facilities, we heated the phosphors at  $1200^\circ\text{C}$  for 2 hrs only. The average crystallite size was calculated from the XRD pattern using Debye Scherer's formula is nano form. Debye Scherer's formula is  $D = K \lambda / \beta \cos\theta$ , Where D = crystallite size for the (hkl), K = constant,  $\lambda$  = X-ray wavelength of incident radiation [CuK $\alpha$  ( $\lambda = 1.54051 \text{ \AA}$ )],  $\beta$  = Full width at half maxima (FWHM),  $\theta$  = Angle of the big peak. Based on the Debye-Scherer's formula, the crystallite size is  $\sim 26.52 \text{ nm}$ . This may conclude that the formation of nano crystallites in the phosphor.

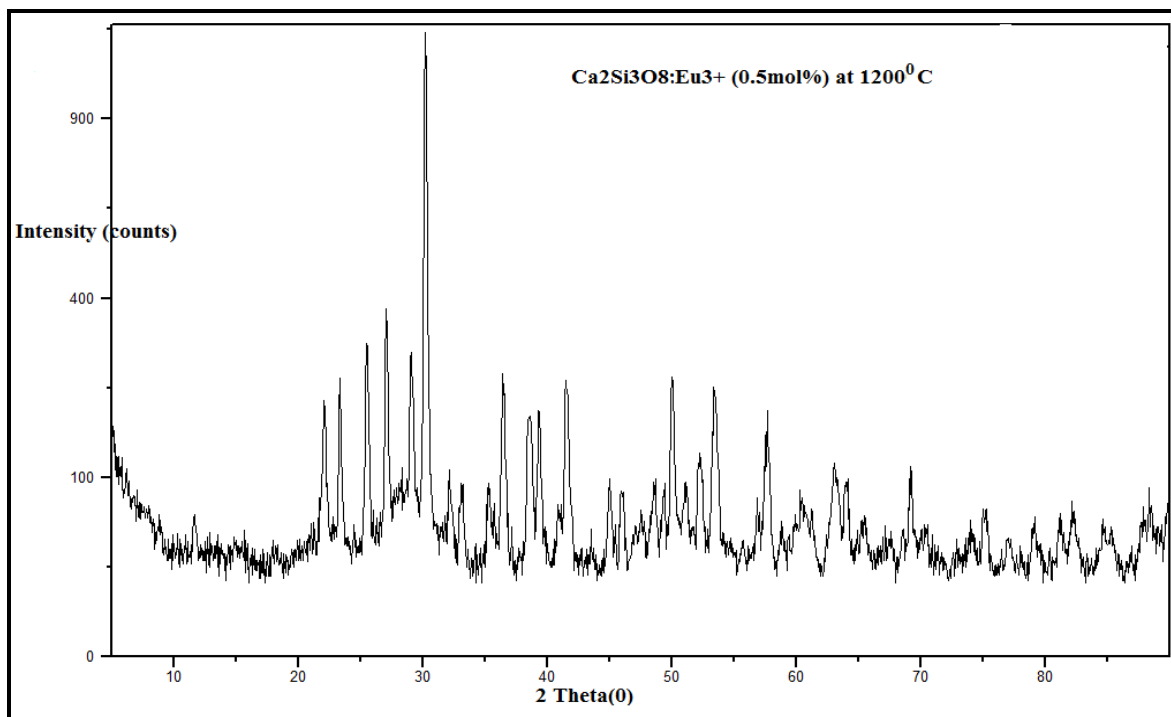


Fig.1:- XRD pattern of  $\text{Ca}_2\text{Si}_3\text{O}_8: \text{Eu}^{3+}$  (0.5mol %) phosphor.

#### Photoluminescence (PL) Analysis:

Figure.2 shows the PL excitation and emissions spectra of  $\text{Ca}_2\text{Si}_3\text{O}_8: \text{Eu}^{3+}$  (0.5mol %) phosphor. From fig.2, it is observed that the excitation spectra are monitored at 400nm wavelength consists of two regions of the broad band which is attributed to charge-transfer (CT) transition from ligand (host) to metal (activator) and shows the peaks at 254 and, 325nm. It can be attributed to f-f transitions. Also observed that, the excitation and emission spectra of  $\text{Ca}_2\text{Si}_3\text{O}_8: \text{Eu}^{3+}$  (0.5mol %) phosphor in the left side shows two excitation spectra (ultra-violet region), resolved at 220-275nm and 300-350nm. The excitation spectrum of  $\text{Ca}_2\text{Si}_3\text{O}_8: \text{Eu}^{3+}$  (0.5mol %) phosphor is complicated to interpret as it depends largely on phase symmetry around the ion. In the present case, the excitation at around 220-275nm is due to the  $\text{Eu}^{3+} - \text{O}_2$  band charge transfer and is closely related to the degree of covalency of the  $\text{Eu}^{3+}$ -ligand bond, as explained by considering  $\text{Eu}^{3+} - \text{O}_2 - \text{Ca}^{2+}$  bonding structure. Since the  $\text{Ca}^{2+}$  ion is a cation with a smaller radius and larger electro-negativity compared to  $\text{Eu}^{3+}$  ion, the electron density clouding around  $\text{O}^{2-}$  ion decreases when it is bonded to  $\text{Ca}^{2+}$  ion [19, 20]. In addition to the prominent excitation peaks due to the excitation from  $^5\text{D}_0$  to  $^7\text{F}_j$  transitions ( $J = 1, 2, 3\dots$ ). The curve second shows small excitations nearly 300-350nm peaking at  $\lambda_{\text{ex}}=325\text{nm}$ .

However from the fig.2 in the right side shows the emission spectra (visible region) observed at  $\lambda_{\text{em}}= 368, 469, 587$  and 612nm peaks respectively. The emission at 368nm peak is due to crystal field and other peaks 469, 587 and 612nm are attributed to  $\text{Eu}^{3+}$  ion transitions due to corresponding the  $^5\text{D}_0 \rightarrow ^7\text{F}_1$  (symmetry sites) and  $^5\text{D}_0 \rightarrow ^7\text{F}_2$  ((hypersensitive to local symmetry) respectively. The amplitude of the 612nm peak is almost larger than the amplitude of 587nm and also very sharper, but both of the prominent emission peaks under the excited at 254, 325nm as shown in fig.2 (a). It is widely known that the main emission peak 612nm due to the electric dipole transition (EDT)  $^5\text{D}_0 \rightarrow ^7\text{F}_2$ , whereas the emission peak 587nm is thought to be due to magnetic dipole transition (MDT) of  $^5\text{D}_0 \rightarrow ^7\text{F}_1$ . It is also believed that the  $^5\text{D}_0 \rightarrow ^7\text{F}_2$  transition is hypersensitive and it depends strongly on local symmetry, whereas the  $^5\text{D}_0 \rightarrow ^7\text{F}_1$  transition is usually insensitivities to site symmetry [21-23]. Interestingly, as shown in this figures 2 & 2(a), both the MDT ( $^5\text{D}_0 \rightarrow ^7\text{F}_1$ ) and EDT ( $^5\text{D}_0 \rightarrow ^7\text{F}_2$ ) spectra are observed in this case. For example, the EDT, at  $\lambda_{\text{em}}=612\text{nm}$  probably arises because of lack of inversion symmetry at the  $\text{Eu}^{3+}$  site. The reason  $^5\text{D}_0 \rightarrow ^7\text{F}_2$  transition is much stronger than  $^5\text{D}_0 \rightarrow ^7\text{F}_1$  transition in that it is usually produced because of the crystal-field splitting of the  $^7\text{F}_2$  level. On the other hand, the MDT,  $^5\text{D}_0 \rightarrow ^7\text{F}_1$ , is insensitive to the site symmetry, and the reason why it has appeared here can be due to the lack of center of symmetry in  $\text{Ca}_2\text{Si}_3\text{O}_8: \text{Eu}^{3+}$  (0.5mol %) phosphor.

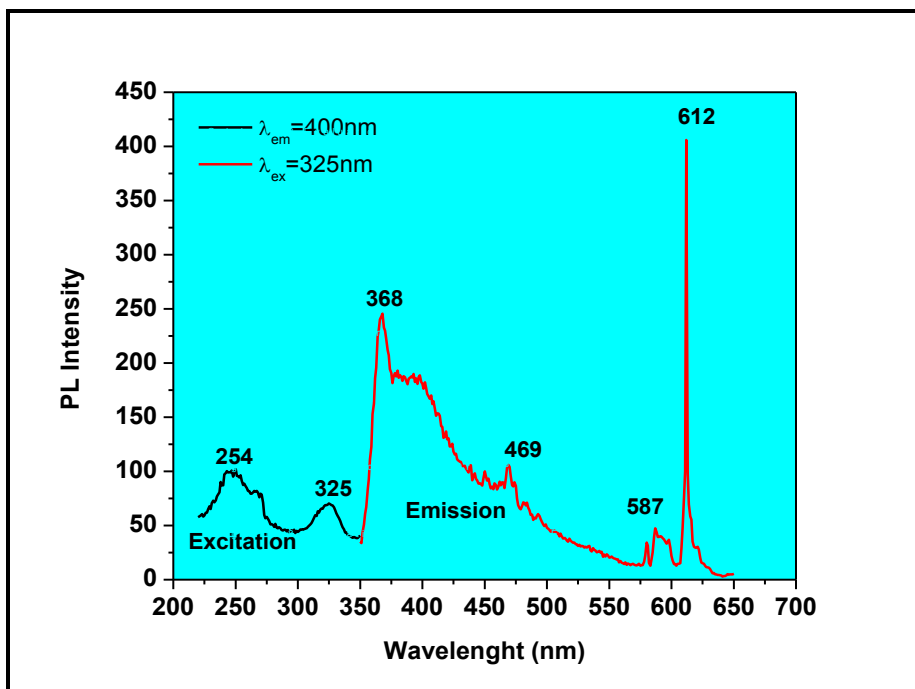


Fig. 2:- PL Excitation and Emission spectra of  $\text{Ca}_2\text{Si}_3\text{O}_8: \text{Eu}^{3+}$  (0.5mol %) phosphor.

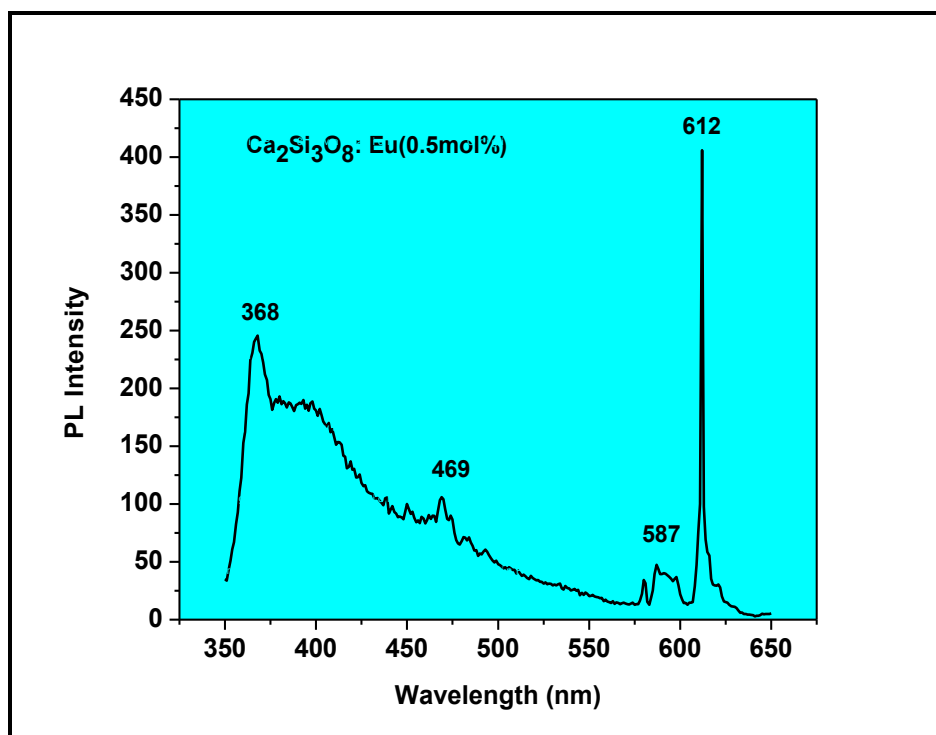
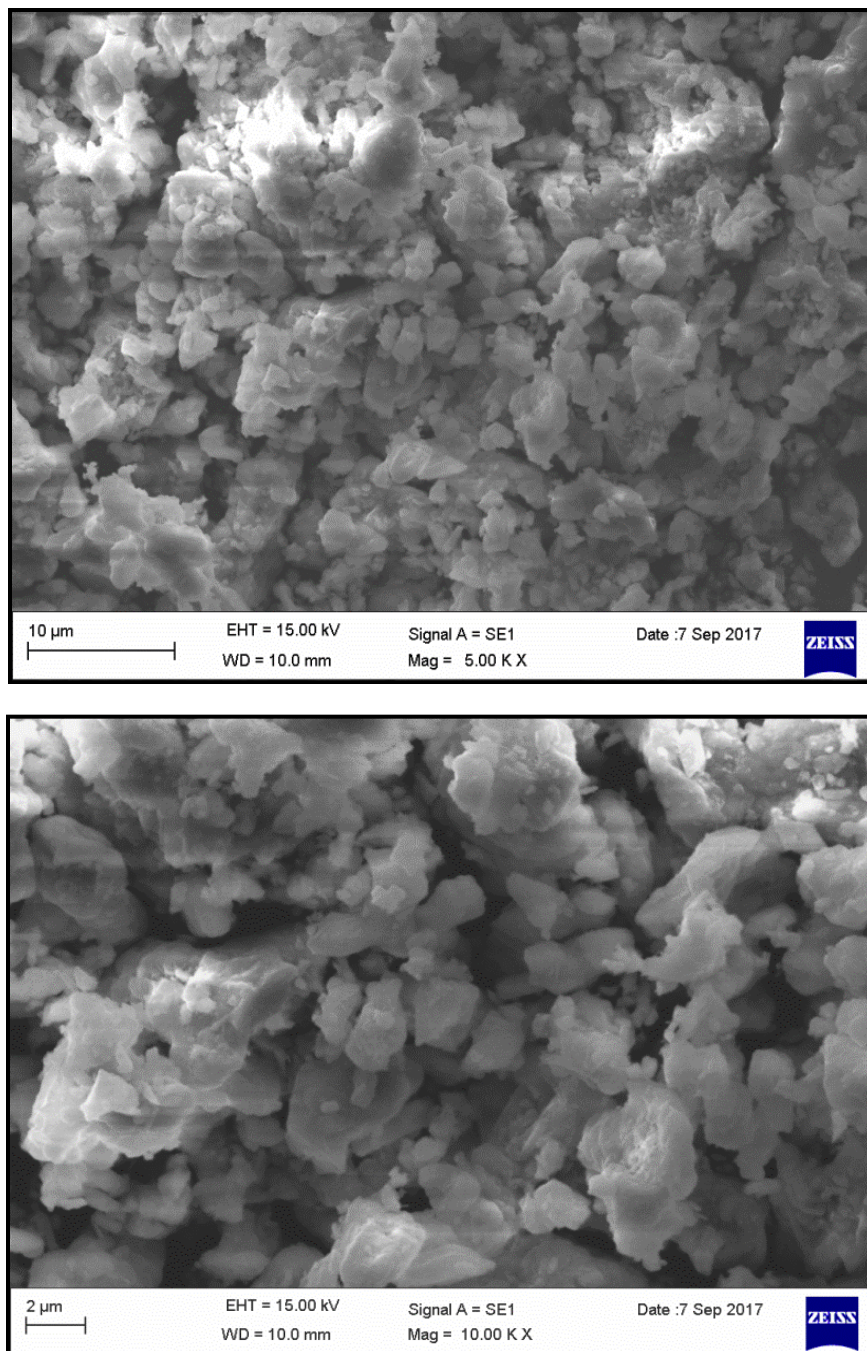


Fig. 2 (a):- PL emission spectrum of  $\text{Ca}_2\text{Si}_3\text{O}_8: \text{Eu}^{3+}$ (0.5mol%) phosphor under excitation 254nm.

#### SEM Analysis:

It is known that the luminescence characteristics of phosphor particles depend on the morphology of the particles, such as size, shape, size distribution, defects, and so on. The surface morphology of the  $\text{Ca}_2\text{Si}_3\text{O}_8: \text{Eu}^{3+}$  (0.5mol %) phosphor is shown in Figure. 3(a) & (b) with different magnification. The surface morphology of the particles was not uniform and they aggregated tightly with each other. From the SEM image, it can be observed that the prepared sample consists of particles with different size distribution fig.3 (a) is  $10\mu\text{m}$  and fig.3 (b) is  $2\mu\text{m}$ . In addition, there

are some big aggregates is also present due to high temperature heat treatment. This confirms formation of very good crystal particles.



**Fig.3 (a) & (b):-SEM image of  $\text{Eu}^{3+}$  (0.5mol %) doped  $\text{Ca}_2\text{Si}_2\text{O}_8$  phosphor under different magnifications**

#### **EDAX Analysis:**

Fig.4 shows the Energy Dispersive through X-ray Analysis (EDAX) of  $\text{Ca}_2\text{Si}_3\text{O}_8: \text{Eu}^{3+}$  (0.5mol %) phosphor. The chemical composition of the powder sample has been measured using EDAX spectra. EDAX is a standard procedure for identifying and quantifying elemental composition of sample area is very small [24]. From the figure.4 & table it is observed that the EDAX containing of element, weight% and atomic% the basic phosphor elements are shown. The existence of Europium (Eu) is clear in their corresponding EDAX spectra. It is concluded that the EDAX figure and table of  $\text{Ca}_2\text{Si}_3\text{O}_8: \text{Eu}^{3+}$  (0.5mol %) phosphor as well as Calcium (Ca), Silicon (Si) and Oxygen (O) of various

percentages are seen which are compared with the calculations made while preparing the phosphors. Therefore it is mainly concluded the formation of the phosphor is as per the empirical formula and weight percentage used to prepare the phosphors using conventional solid state reaction (SSR) method. It is also concluded the SSR method is to synthesize the phosphors under study is a very good method.

Element	Weight %	Atomic %
O K	52.64	69.99
Si K	21.58	16.34
Ca K	25.76	13.67
Eu L	0.02	0.00
Totals	100.00	

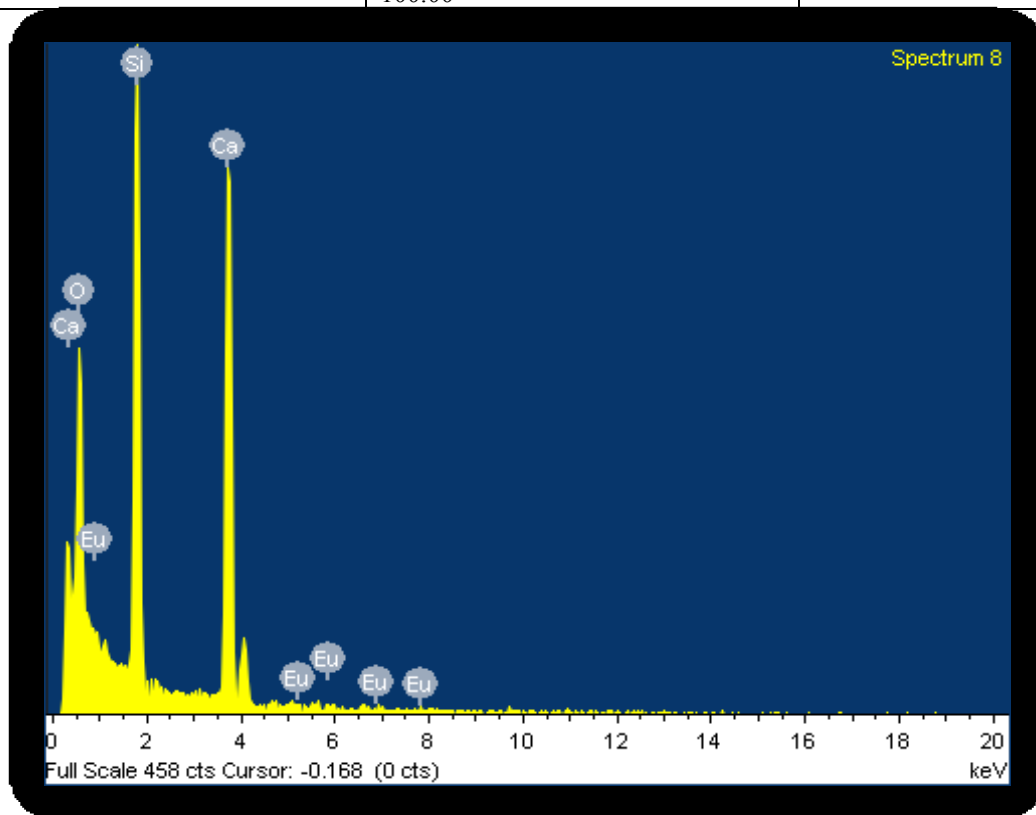


Fig. 4:- EDAX Spectra of  $\text{Eu}^{3+}$  (0.5mol %) doped  $\text{Ca}_2\text{Si}_2\text{O}_8$  phosphor.

#### CIE Analysis:

The CIE co-ordinates were calculated by the Spectrophotometric method using the spectral energy distribution. The luminescence color co-ordinates of [ $\text{Eu}^{3+}$  (0.5mol %) doped  $\text{Ca}_2\text{Si}_2\text{O}_8$  phosphor] the sample excited under 254 & 325nm has been characterized by the CIE (Commission International de l'Eclairage) 1931-colour chart chromaticity diagram [25]. Fig.5 shows the color co-ordinates emission spectrum of the  $\text{Eu}^{3+}$  (0.5mol %) doped  $\text{Ca}_2\text{Si}_2\text{O}_8$  phosphor was converted to the CIE 1931-colour chart chromaticity using the CIE software from Radiant Imaging. Points (i) & (ii) are  $x = 0.658$  and  $y = 0.313$  indicates red colour ( $\lambda_{\text{em}} = 612\text{nm}$ ) under 254 & 325nm excitation wavelengths.

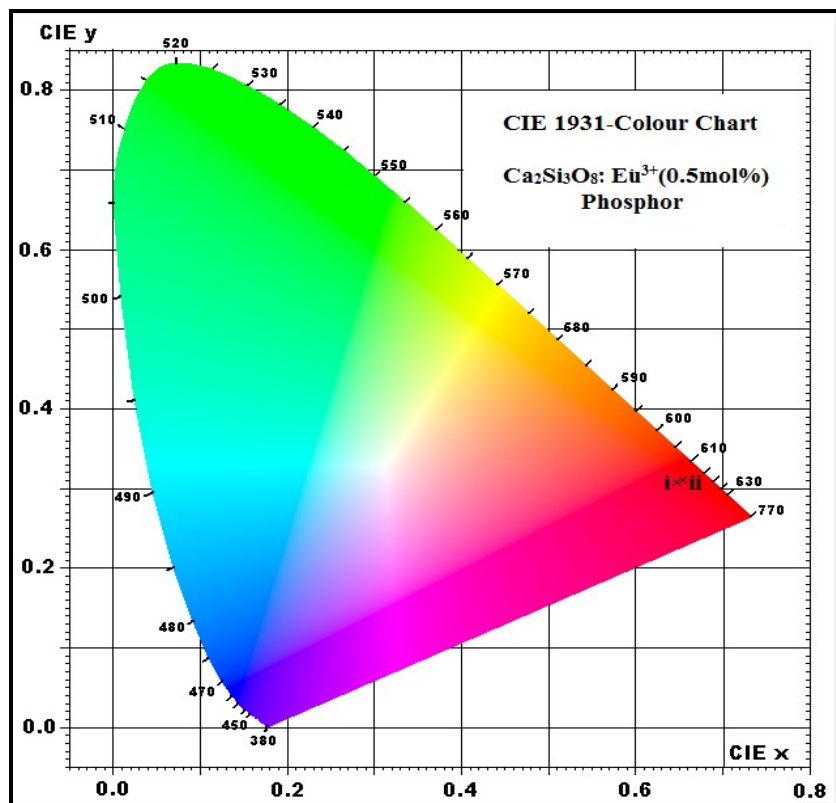


Fig.5:- CIE co-ordinates of  $\text{Eu}^{3+}$  (0.5mol %) doped  $\text{Ca}_2\text{Si}_2\text{O}_8$  phosphor.

### Conclusion:-

1. Photoluminescence properties of  $\text{Eu}^{3+}$  (0.5mol%) doped  $\text{Ca}_2\text{Si}_2\text{O}_8$  phosphor materials were strongly influenced by the doping of activator ion ( $\text{Eu}^{3+}$ ) ion. From the luminescence spectra of these phosphors, it was found that  $\text{Eu}^{3+}$  (0.5mol%) concentration is provided maximum photoluminescence response.
2. Luminescence emission spectra of prepared materials showed intense red color with 254,325nm excitation. Strong intense peak of these light emitting materials was located in 610-615 nm regions due to  $^5\text{D}_0 \rightarrow ^7\text{F}_2$  transition of  $\text{Eu}^{3+}$  ion. Maximum luminescence intensity of the phosphors was obtained when these materials were heated at 1200°C was sufficient.
3. It is widely known that the main emission peak 612nm due to the electric dipole transition (EDT)  $^5\text{D}_0 \rightarrow ^7\text{F}_2$ , whereas the emission peak 587nm is thought to be due to magnetic dipole transition (MDT) of  $^5\text{D}_0 \rightarrow ^7\text{F}_1$ . It is also believed that the  $^5\text{D}_0 \rightarrow ^7\text{F}_2$  transition is hypersensitive and it depends strongly on local symmetry, whereas the  $^5\text{D}_0 \rightarrow ^7\text{F}_1$  transition is usually insensitivities to site symmetry.
4. The average crystallite size was calculated from the XRD pattern using Debye Scherer's formula is nano form. Debye Scherer's formula is  $D = K \lambda / \beta \cos\theta$ , Where  $D$  = crystallite size for the (hkl),  $K$  = constant,  $\lambda$  = X-ray wavelength of incident radiation [CuK $\alpha$  ( $\lambda = 1.54051 \text{ \AA}$ )],  $\beta$  = Full width at half maxima (FWHM),  $\theta$  = Angle of the big peak. Based on the Debye-Scherer's formula, the crystallite size is  $\sim 26.52 \text{ nm}$ . This may conclude that the formation of nano crystallites in the phosphor.
5. From the SEM image, it can be observed that the prepared sample consists of particles with different size distribution fig.3 (a) is  $10 \mu\text{m}$  and fig.3 (b) is  $2 \mu\text{m}$ . In addition, there are some big aggregates is also present due to high temperature heat treatment. This confirms formation of very good crystal particles.
6. Fig.4 shows the Energy Dispersive through X-ray Analysis (EDAX) of  $\text{Ca}_2\text{Si}_3\text{O}_8: \text{Eu}^{3+}$  (0.5mol %) phosphor. Therefore it is mainly concluded the formation of the phosphor is as per the empirical formula and weight percentage used to prepare the phosphors using conventional solid state reaction (SSR) method. It is also concluded the SSR method is to synthesize the phosphors under study is a very good method.
7. Finally, this phosphor can be a promising candidate for the generation of red light in solid state lightning and also in the field of display devices.

**Acknowledgment:-**

1. One of the authors (Ch. Atchyutha Rao) is very grateful for the financial support from the University Grant Commission (UGC), New Delhi, India, under Minor research **Project (MRP No: 4687/14-SERO/UGC)**. And also thankful to the Principal and Bapatla Educational Society of the Bapatla College of Arts & Sciences, Bapatla for continues encouragement during this project work.

**References:-**

1. X. Sun, J. Zhang, X. Zhang, S. Lu, X. Wang, J. Lumin., 122–123 (2007) 955
2. S.P. Lee, T.S. Chan, T.M. Chen, ACS Appl. Mater. Interfaces, 7(1) (2015) 40
3. J.S. Kim, H.J. Song, H.S. Roh, D.K. Yim, J.H. Noh, K.S. Hong, Mater. Lett., 79 (2012) 112
4. W. Pan, G. Ning, J. Wang, Y. Lin, J. Ye, J. Lumin., 129(5) (2009) 584
5. Z. Chen, J.H. Zhang, S. Chen, M.Y. Lin, Zou, K. Guo, J. Alloys Compd., 632 (2015) 756
6. W. Lv, N. Guo, Y. Jia, Q. Zhao, H. You, Opt. Mater., 35(5) (2013) 1013
7. X. Luo, W. Cao, F. Sun, Chin. Sci. Bull., 53(19) (2008) 2923
8. S.J. Dhoble, S.K. Raut, N.S. Dhoble, Int. J. Lumin and Appln, 5(2) (2015) 178
9. Y. Zhang, X. Li, K. Li, H. Lian, M. Shang, J. Lin, ACS Appl. Mater. Interfaces, 7 (2015), 2715
10. D. Singh, V. Tanwar, S. Bhagwan, S. Sheoran, V. Nishal, J. Nanoelectron. Optoelectron., 10 (2015) 01
11. V.R. Bandi, Y.T. Nien, T.H. Lu, I.G. Chen, J. Am. Ceram. Soc., 92(12) (2009) 2953
12. M.R. Kadukar, P.W. Yawalkar, J. Biolumin. Chemilumin., 30(8) (2015) 1219
13. J.K. Park, K.J. Choi, H.G. Kang, J.M. Kim, C.H. Kim, Electrochem, Solid-State Lett., 10(2) (2007) J15
14. V.R. Bandi, B.K. Grandhe, K. Jang, H.S. Lee, S.S. Yi, J.H. Jeong, Ceram. Int., 37(6) (2011) 2001
15. K.V. Ivanovskikh, A. Meijerink, F. Piccinelli, C. Ronda, M. Bettinelli, J. Lumin., 130(5) (2010) 893
16. F. Piccinelli, A. Speghini, G. Mariotto, L. Bovo, M. Bettinelli, J. Rare Earths, 27(4) (2009) 555
17. R. Krsmanovic, Z. Antic, I. Zekovic, M. D. Dramicanin, J. Alloys Compds, 480 (2009) 494–498
18. H. Chang, H. D. Park, K. S. Sohn, J. D. Lee, J. of the Korean Phys. Soc., 34 (1999) 545-548
19. L. Lin, C. Shi, Z. Wang, W. Zhang, M. Yin, J. of Alloys and Compds., 466 (2008) 546–550
20. L. Yang, M. Fang, L. Du, Z. Zhang, L. Ren, X. Yu, Mater. Res. Bull., 43 (2008) 2538–2543
21. J. Yang, Z. Quan, D. Kong, X. Liu, J. Lin, Cryst. Growth and Des, 7 (2007) 730-735.
22. Q. Yanmin, Z. Xinbo, Y. Xiao, C. Yan, G. Hai, J. Rare Earths, 27 (2009) 323-326.
23. Lei Zhou, Bing Yan, J. Phys. Chem., Solids 69 (2008) 2877–2882
24. D.V. Sunitha, H. Nagabhushana, F. Singh, S.C. Sharma, J. Lumin., 132 (2012) 2065–2071.
25. Color Calculator version 2, software from Radiant Imaging, Inc, 2007.